

Article

The Effects of Indium Additions on Tribological Behavior of Spark Plasma Sintering-Produced Graphene-Doped Alumina Matrix Composites for Self-Lubricating Applications

Viktor Puchý , Mária Podobová , Richard Sedlák * , Ladislav Falat , Róbert Džunda , František Kromka and Ján Dusza

Institute of Materials Research SAS, Watsonova 47, 04001 Košice, Slovakia; vpuchy@saske.sk (V.P.)

* Correspondence: rsedlak@saske.sk; Tel.: +421-55-792-2400

Abstract: Alumina (Al_2O_3) ceramics are interesting for low-weight and mid-high temperature applications. The addition of indium (In) and graphene nanoplatelets (GNPs) can be used to reduce the density and modify the functional properties and mechanical performance of the ceramic matrix. GNP and In-reinforced Al_2O_3 matrix composites were prepared by the spark plasma sintering (SPS) technique. Monolithic Al_2O_3 and Al_2O_3 matrix composites with either 5 or 10 wt.% of In and 2 wt.% of GNPs (Al_2O_3 -5In-2GNPs and Al_2O_3 -10In-2GNPs) were compacted into disc-shaped samples. The microstructure was studied and characterized with light-optical microscopy (LOM) and scanning electron microscopy (SEM). Hardness was determined using the Vickers technique and tribological properties were studied by the ball-on-disk method. The coefficient of friction (COF) and specific wear rates were evaluated from tribological tests. Worn surfaces were studied by SEM and confocal microscopy. Interdiffusion transition regions were formed among individual microstructural constituents (Al_2O_3 , In, GNPs) under high sintering temperatures, which were responsible for the balanced hardness and low porosity of the produced composites. The addition of In and graphene nanoplatelets resulted in smaller COF and wear rates indicating good improvement in the tribological behavior. The prepared Al_2O_3 -5In-2GNP and Al_2O_3 -10In-2GNP composites represent promising nanocomposites for self-lubricating applications.

Keywords: alumina; graphene nanoplatelets; indium; spark plasma sintering; COF; wear



Citation: Puchý, V.; Podobová, M.; Sedlák, R.; Falat, L.; Džunda, R.; Kromka, F.; Dusza, J. The Effects of Indium Additions on Tribological Behavior of Spark Plasma Sintering-Produced Graphene-Doped Alumina Matrix Composites for Self-Lubricating Applications. *Crystals* **2024**, *14*, 104. <https://doi.org/10.3390/cryst14010104>

Academic Editor: Pavel Lukáč

Received: 29 December 2023

Revised: 11 January 2024

Accepted: 13 January 2024

Published: 22 January 2024



Copyright: © 2024 by the authors. Licensee MDPI, Basel, Switzerland. This article is an open access article distributed under the terms and conditions of the Creative Commons Attribution (CC BY) license (<https://creativecommons.org/licenses/by/4.0/>).

1. Introduction

Aluminum oxide is used widely in materials science, especially in the field of ceramics as it can be used in ceramics, polishing and abrasive applications, etc. Alloys based on aluminum oxides, including their composites, have a very wide range of uses in industrial practice. It is their low weight and excellent mechanical properties that support the possibilities of their use, ranging from electronics to space technologies [1]. Over the years of research into aluminum oxide, and other structural ceramics, these materials have been improved by the addition of various constituents into their matrix to improve their mechanical, electrical, and tribological properties. Graphene has become the most promising and mainly used material to achieve improvement in these properties. Most of the studies were focused on improving the electrical conductivity and the fracture toughness of the ceramic matrix by adding graphene as a nanofiller, because of its superior electrical conductivity [2–5]. As friction is one of the major forms of energy loss and, to a lesser extent, material loss, it is/was necessary to find suitable mechanisms for lowering these losses. By focusing on the mechanical and tribological properties, it has been reported that graphene has also proven to be an excellent lubricant additive due to its two-dimensional layered structure [6–13]. Graphene is a good candidate for solid lubrication that reduces the friction force between contact surfaces at micro- and nanoscale while protecting the coated surface by forming a carbon-rich tribo-film acting as a lubricant and protection on

contact surfaces [14–16]. Research has shown that even at relatively low contents, graphene can significantly improve tribological properties [17,18]. It is added to the ceramic matrix in various forms, such as graphene oxide (GO), reduced graphene oxide (rGO), exfoliated graphene sheets, graphene nanoplatelets (GNPs), or carbon nanotubes or nanofibers (CNTs, CNFs). Kim et al. [13] investigated Al_2O_3 with graphene after sintering at low pressure. They achieved an order-of-magnitude increase in wear resistance even under normal load (25N) caused by the tribo-effect of graphene, even with the proportion of ultra-thin graphene (0.25–0.5 vol.%). However, in another study, a striking effect of graphene was revealed at about 10 vol.%. Solid lubricants have promising potential to replace liquid lubricants in cases where it is necessary to prevent their sublimation, especially for applications in vacuum, space, and other extreme conditions. The replacement of liquid and grease lubricants with solid lubricants is/was carried out in practice by applying coatings by chemical or physical vaporizing to create a solid lubricating layer, but these have a limited lifetime, poor adhesion, with difficulties in replenishment, oxidation, and aging-related degradation [19]. Therefore, research efforts have been focused on adding toughening and lubricating fillers into the matrix. The research focused on the use of carbon materials in various forms (CNT, CNE, GO, rGO, ...) and the result was the self-lubricating ability of aluminum-metal matrix composites with added graphene [20]. Increasing demands for the lowest possible friction losses in various applications force research to be increasingly focused on self-lubricating materials [21,22], which are expected to provide excellent tribological properties under extreme conditions. In addition to methods of adding solid self-lubricating materials onto various functional surfaces (magnetron sputtering, laser cladding, thermal spraying, and vapor deposition techniques), powder metallurgy is a method of incorporating solid lubricants into a matrix [23–34]. There are several types of solid lubricants used for self-lubricating materials; among them are soft metals such as Ag, Sn, Au, Pb, In, Pt, etc., exhibiting multiple slip planes. The destruction of lattice defects, such as dislocations and vacancies, results in improper work hardening, leading to excellent lubricity under extreme conditions [35]. Puchy et al. [36] published a work devoted to the tribological properties of composites based on Si_3N_4 with the addition of graphene and silver, prepared by SPS. As a result, silver in combination with GNPs improved the sintering ability, and limited the occurrence of sintering-related structural defects, thus neither pores nor microcracks were observed in the material. The COF decreased from 0.63 to 0.57 with the addition of 5 vol.% Ag compared to monolithic Si_3N_4 . Wardzinski et al. [37] investigated the possibilities of replacing lead with indium. Lead is used for its operating life in a vacuum. However, lead is toxic, so its use has been limited in recent years and replacements suitable for use in applications in extreme conditions are being sought. Their research results show that PVD-indium coating exhibits very low in-vacuum friction compared to that with lead.

The aim of the present work is to explore the possibilities of using indium as a solid lubricant in an alumina matrix with the addition of graphene nanoplatelets (GNPs) and to create a ceramic–metal composite with the ability of self-lubrication and promising potential for use/application in extreme conditions. The samples of Al_2O_3 -In-GNPs composites, prepared by the SPS technique, were subjected to tribological tests and microstructural analyses in order to investigate the effects of indium additions to Al_2O_3 /GNP composites on their resulting tribological behavior in correlation with observed wear mechanisms.

2. Materials and Methods

Commercial pure aluminum oxide, α -phase < 1.0 micron powder with purity 99.9% was used as the matrix material and was obtained from Thermo Scientific Chemicals, ThermoFisher (Kandel) GmbH, Kandel, Germany. Also materials graphene nanoplatelets aggregates S.A. 500 m^2/g , sub-micronparticles powder and Indium powder, -325 mesh, Puratronic™, purity 99.995% were supplied by Thermo Scientific Chemicals, ThermoFisher (Kandel) GmbH Germany. The prepared powders were mixed and homogenized in a 3D Turbula mixer (WAB AG, Muttenz, Switzerland) for 60 min at 30 rpm under an air

atmosphere. Tungsten carbide balls with a diameter of 10 mm were used in the mixing and homogenizing process. Ball-to-powder weight ratio was selected to be 5:1. The SPS (Type HP D 10SD, FCT Systeme, Frankenblick, Germany) with a graphite tool assembly was used to produce specimens with a processing temperature of 1750 °C and a maximum sintering pressure of 62.8 MPa in a vacuum 5 Pa. As shown in Figure 1, specimens were heated to 1750 °C within 12 min, followed by 10 min of holding at peak temperature and a controlled cooling step within 12 min. For comparison, a pure alumina sample was also fabricated under the same conditions. The final samples had a disc shape with circa 3 mm thickness and 20 mm in diameter. The relative densities of the sintered samples were determined by the Archimedes method with deionized water. First, the weight of the samples was measured in air and then in water, and then the difference between the two weights was calculated. The relative density was then calculated by dividing the weight of the object in air by the difference between the weight of the object in air and the weight of the object in water.

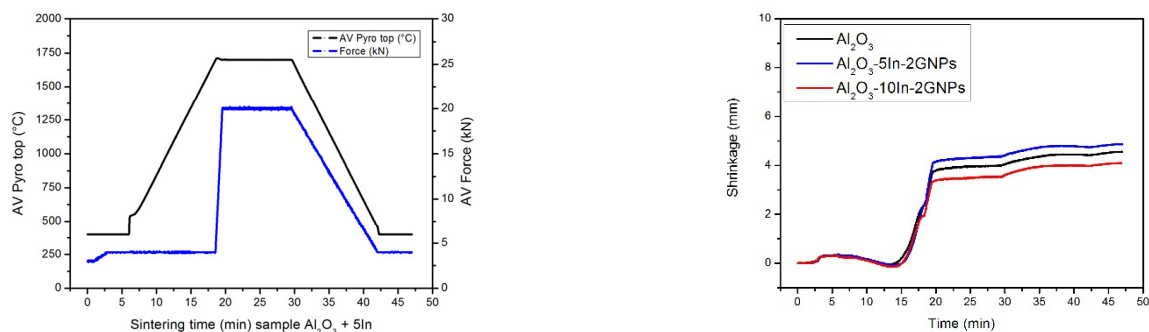


Figure 1. Sintering curves as well as punch displacement (shrinkage) plots of the monolith and composites containing 5 wt.% and 10 wt.% In, with maximum load of 20 kN equaling an applied pressure of 62.8 MPa.

The sintered samples were embedded in the conductive resin. Next, the surfaces of the samples were ground and mechanically polished using colloidal diamond suspensions (from 30 to 1 µm). The microstructure observations of specimens prepared in this way were carried out using a light optical microscope (LOM) OLYMPUS GX71 (Olympus Corporation, Tokyo, Japan) equipped with a digital camera. The local microstructures were observed using the scanning electron microscope (SEM) JEOL JSM-7000F (Jeol Ltd., Tokyo, Japan). The observations were performed with the use of backscattering electron (BSE) mode.

The average grain size of each composite was determined using the line method on scanning electron microscopy (SEM) images. The microhardness (HV1) was measured according to standard methods for ceramics, ASTM C1327 (Standard Test Method for Vickers Indentation Hardness of Advanced Ceramics). For measuring the indentation hardness of prepared samples, we selected this method because Vickers indentations are influenced less by specimen surface flatness, parallelism, and surface finish than Knoop indentations. Microhardness was determined by Vickers indentation (Wilson 1102/1202 Vickers Hardness Tester) under the load of 1 N with a dwell time of 10 s at the maximum load. At least a set of 10 indents per specimen was introduced. Then, the average value was calculated and its standard error was also calculated. Tribology tests were performed on HTT automatic tribometer (CSM instruments, Switzerland) in rotational dry sliding conditions, using ball-on-disc geometry, at room temperature and pressure. A SiC ceramic ball with a 6 mm diameter was used as a tribological partner. The number of samples for friction and wear measurements was one from each kind. All tests were carried out under 2 N normal load, 0.1 m/s sliding velocity, and 5 mm track radius. The total sliding distance was 300 m. The coefficient of friction (COF) was calculated by taking the ratio of the tangential and normal forces and it was reported versus the sliding distance. Topographical measurements of tribological profiles and specific wear rate determination were performed

using a confocal microscope PLu neox 3D Optical Profiler (SENSOFAR, Barcelona, Spain). The wear rate, W , was determined in terms of the volume loss V per distance L and applied load F according to the following equation:

$$W = \frac{V}{L \times F} \quad (1)$$

3. Results and Discussion

Sintering curves as well as punch displacement (shrinkage) plots of the monolith and composites are shown in Figure 1. The samples were heated with a heating rate of 100 °C/min. Four regions were detected in the shrinkage. In the first region with the temperature below 1500 °C, no changes were detected in the shrinkage of any samples. Shrinkage of the samples started in the second region between 1500 °C and 1625 °C. This displacement may be due to various reasons such as particle rearrangement, plastic deformation of the metallic phase, formation of a liquid phase, plastic deformation of graphite foils, and sintering, and a reduction in the porosities. In the third region, a relatively sharp displacement could be observed, related to increasing the uniaxial pressure from 4 kN to 20 kN at 1625 °C. In the fourth region related to the dwell time at a maximum sintering temperature of 1750 °C, the minimum value of the displacement changes could be observed which indicated the complete densification of the samples.

The analysis of the X-ray spectra obtained from the sintered materials in disc form revealed the presence of strong characteristic peaks located at 2θ angles, which corresponded to the alumina, indium, and carbon phases (Figure 2). In particular, the alumina matrix and the indium-graphene reinforced composites were compared.

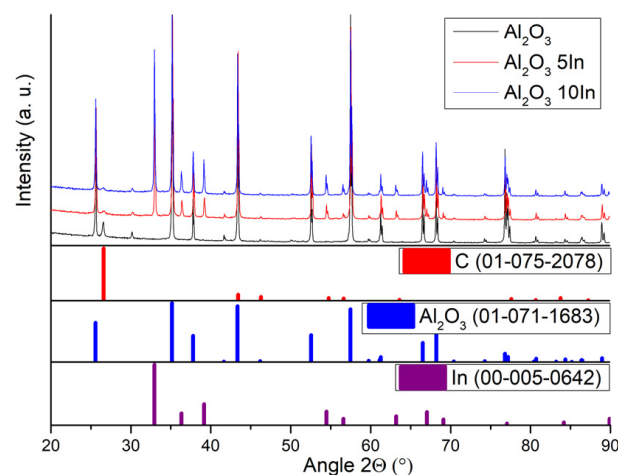


Figure 2. X-ray diffraction spectra of sintered Al₂O₃, Al₂O₃-5In-2GNP composite, and Al₂O₃-10In-2GNP composite.

The microstructures of monolithic Al₂O₃, Al₂O₃-5In-2GNP, and Al₂O₃-10In-2GNP composites produced by the SPS method were examined by Jeol SEM examination (Figure 3). Microstructural analysis showed that in the monolithic Al₂O₃ material, a dense microstructure with very low porosity was found. In the Al₂O₃-5In-2GNP composite material, the relatively homogenous distribution of In and GNPs was determined. According to analyses (Figure 4), it was observed that In has a globular shape located between grains and GNPs are distributed around individual grains which can enhance the sintering process. It seemed that, in some local regions, there was no adequate homogeneous distribution. It was observed that the In and GNP elements clustered towards the grain boundaries.

The performed investigations indicated that changes in the amount of indium powder directly affected the decrease in the hardness of the spark plasma sintered composites (Figure 5). The hardness measurements showed that the decrease in the hardness was almost

linear. For the lower value (5 wt.%), the obtained hardness was 12.83 ± 1.84 GPa, while the 10 wt.% of added indium powder led to a hardness decrease even to 9.90 ± 2.67 GPa, respectively. According to the literature, theoretically, Vickers hardness of alumina ceramic (99.0% Al_2O_3) is about 10 GPa and depends on the sintering process and powder purity (grades). The experiments also revealed that Al_2O_3 -5In-2GNP spark plasma sintered composites produced with 5 wt.% of indium powder were characterized by a slightly lower density. The rise in incorporated indium metal caused the formation of a less dense microstructure. The relative density of the samples, calculated according to Archimedes principle, was approximately 97.6%, 95.7%, and 93.2%, respectively (Figure 5).

The obtained results showed that incorporating metal particles and carbon nanoparticles like indium and graphene nanoplatelets had a significant influence on matrix microstructure, its hardness, and defect formation, such as cracks and porosity. The literature data indicate that the COF of alumina–graphene composite materials prepared with the use of the SPS method and similar process parameters was approximately two times higher but wear was considerably lower compared to our composites. It could be due to the fact that the composites obtained by Gutierrez-Gonzalez et al. [38] had a graphene concentration in the composite of only 0.22 wt.%.

In alumina composite samples, a mechanical mixing time of 0.5 h was chosen to ensure that the In and GNPs particles were dispersed as homogeneously as possible in the alumina matrix. It was observed in the previous study that if the GNP ratio in ceramic composites exceeds 1 wt.%, the graphene particles may create clusters in the structure and cause agglomeration [19].

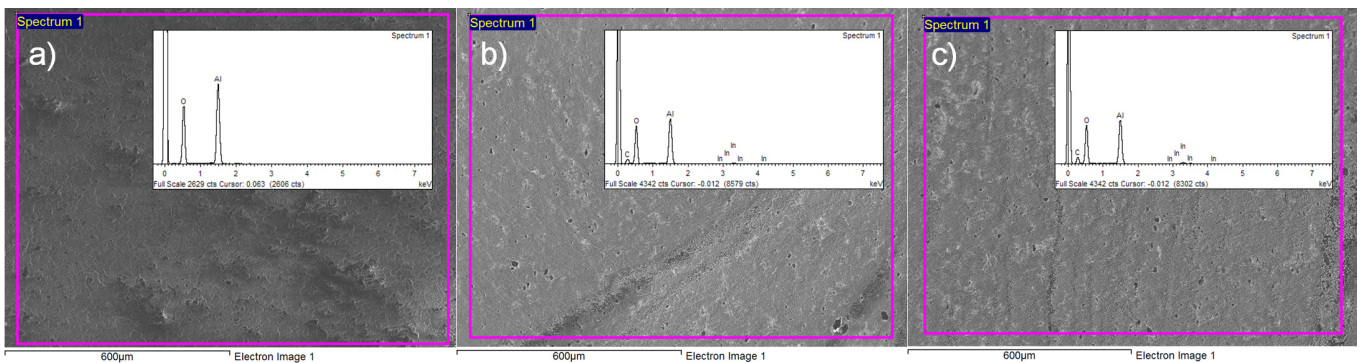


Figure 3. SEM-EDS micrographs on Al_2O_3 (a), Al_2O_3 -5In-2GNP composite (b), and Al_2O_3 -10In-2GNP composite (c).

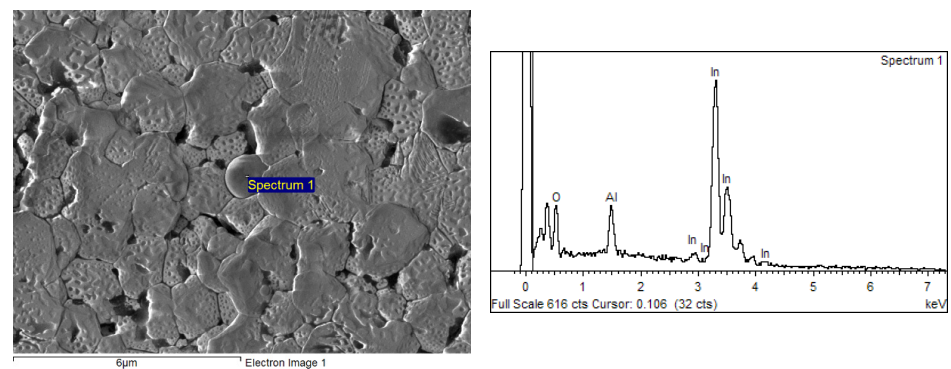


Figure 4. Cont.

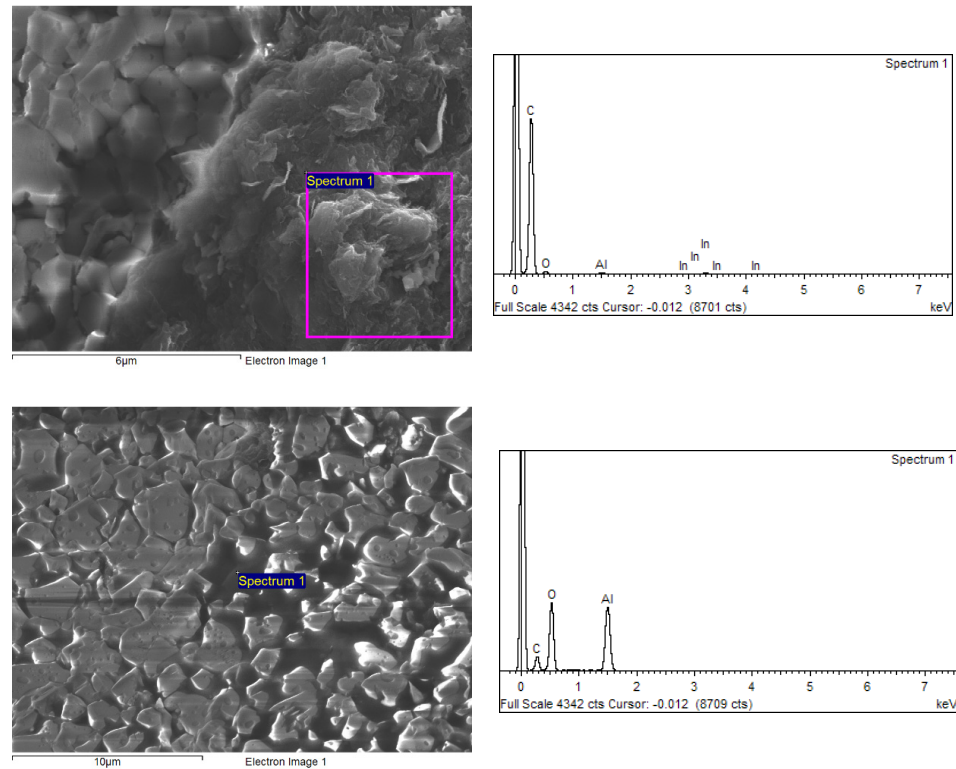


Figure 4. SEM–EDS micrographs on composites.

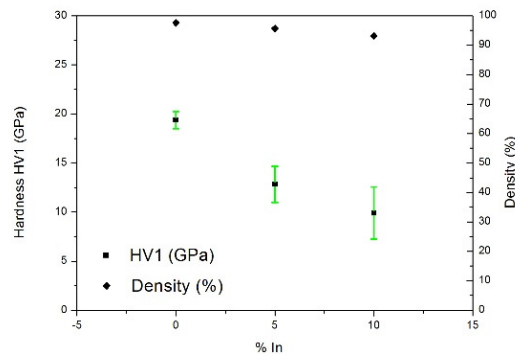


Figure 5. Hardness and density of samples.

To achieve high performance and better friction properties in alumina composites, it is desirable that the reinforcement particles should be distributed as homogeneously as possible in the matrix, and a good interface bond should also be formed between the reinforcement particles and the matrix. To increase the homogeneity, the mechanical mixing time can be increased, and the ball-to-powder ratio can be changed to eliminate undesirable problems such as low hardness, poor sintering, and poor wear resistance in the mechanical and tribological properties of the composites. Figure 6 shows the microscopic morphology on the sliding surface of the Al_2O_3 , Al_2O_3 -5In-2GNP, and Al_2O_3 -10In-2GNP composites. In Figure 7, the element distribution of the SEM-EDS analysis of the composites is shown. It should be pointed out that red, green, blue, dark blue and yellow color areas correspond to the phases of Al_2O_3 , In, SiC, and graphene nanoplatelets, respectively.

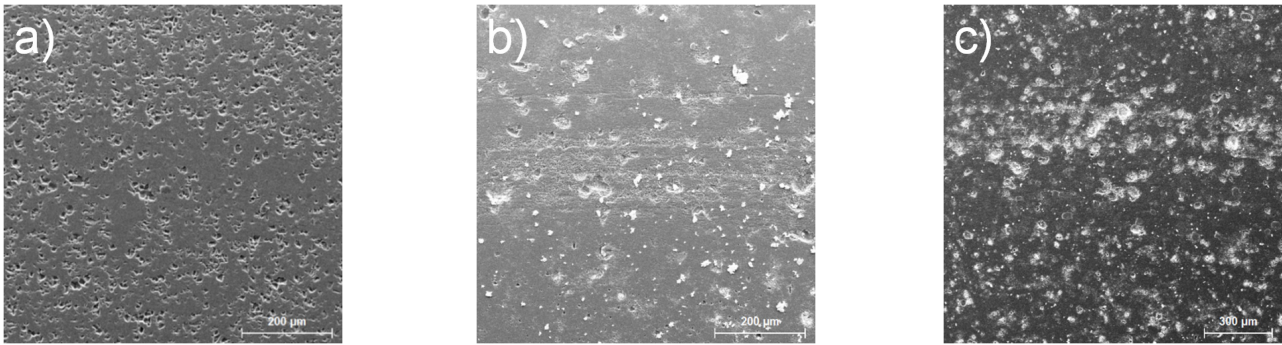


Figure 6. SEM microscopic morphology on the sliding surface of Al₂O₃ (a), Al₂O₃-5In-2GNP composite (b), and Al₂O₃-10In-2GNP composite (c).

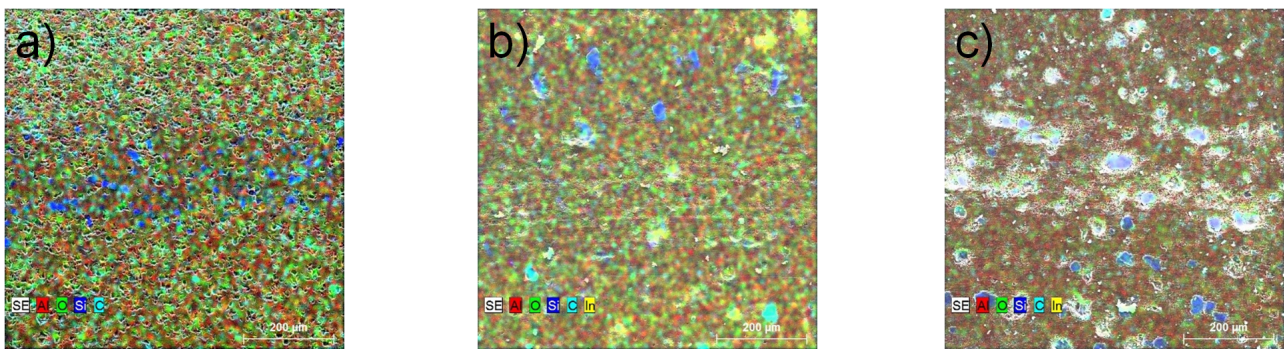


Figure 7. SEM micrographs with EDS analyses of wear tracks on Al₂O₃ (a), Al₂O₃-5In-2GNP composite (b), and Al₂O₃-10In-2GNP composite (c) at a rotational speed of 0.1 m/s, length of 300 m and friction force of 2 N, obtained from tests under dry conditions.

The SiC ball was used for the ball-on-disc friction test as a friction partner. The ball radius was 6mm. The length of the friction track on the surface was set at 300 m in all samples. The measured widths of the friction traces on the surface were 420, 380, and 390 μm, respectively. The pitting depths in the friction traces of the composites were from about 3 up to 9 μm, which were little more than those of monolith (3 μm). In order to investigate the wear and friction, the wear rate was also calculated. Figure 8 shows the coefficients of friction and wear rates of the investigated materials. It can be seen that the wear rates of the prepared composites Al₂O₃-5In-2GNPs (36.21×10^{-6} [mm³/m.N]) and Al₂O₃-10In-2GNPs (14.34×10^{-6} [mm³/m.N]) were less than that of the monolithic material (31.71×10^{-6} [mm³/m.N]). The wear rate of the Al₂O₃-10In-2GNP composite was only 45% of the monolith material wear rate. This indicates that the Al₂O₃-10In-2GNP composite had better wear resistance. The main reason was that the GNP particles could form the toughened ceramic matrix, and the added Indium metallic particles could form a friction film. There was still a small amount of free GNP particles between the crystals (Figure 4). These phases increased the wear resistance due to the self-lubricating indium coating created. Figure 8 shows the COF of the of Al₂O₃, Al₂O₃-5In-2GNP, and Al₂O₃-10In-2GNP composites at the rotational speed of 0.1 m/s, length of 300 m, and friction force of 2 N, obtained from tests under dry conditions. The COF of the Al₂O₃ substrate was in the range of 0.2–0.45, and it was usually around 0.43. This friction coefficient became stable after 150 m. The COF of the Al₂O₃-5In-2GNP composite was in the range of 0.2–0.38, and it was usually around 0.35. After 200 m, the friction coefficient became stable. In the case of the Al₂O₃-10In-2GNP composite, the COF was in the range of 0.2–0.35, and it was usually around 0.33 and after 50 m became stable. It can be seen that the Al₂O₃-10In-2GNP composite had a smaller coefficient and more stable fluctuations. This indicates that the indium friction film and small GNP particles made the friction and wear between the SiC ball and alumina-based matrix smaller.

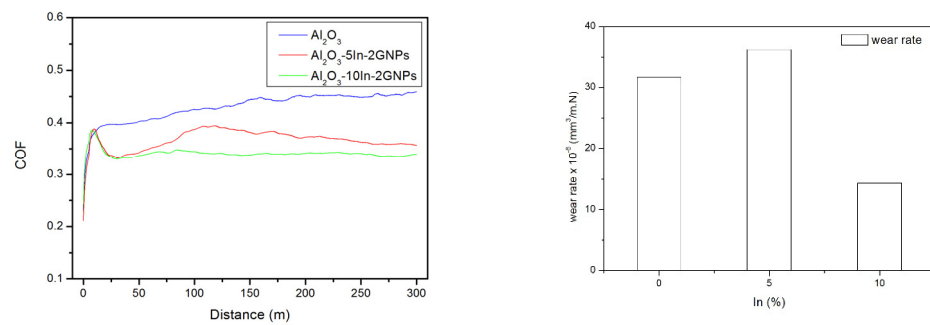


Figure 8. COF vs. time and wear rate graphs of Al₂O₃, Al₂O₃-5In-2GNP, and Al₂O₃-10In-2GNP composites at the rotational speed of 0.1 m/s, a length of 300 m and friction force of 2 N, obtained from tests under dry conditions.

Figures 6 and 7 show the microscopic morphology on the sliding surface of the Al₂O₃, Al₂O₃-5In-2GNP, and Al₂O₃-10In-2GNP composites. In Figure 7a, there were some spalling zones with a small area and shallow furrows on the sliding surface. The main wear mechanism of the monolithic alumina was mainly adhesive and less abrasive wear. In Figure 7b,c, it can be seen that there were some spalling zones with a large area and deep furrows on the sliding surface of the composites. The main wear mechanism of the substrate was mainly abrasive and less adhesive wear.

The added In and GNP particles provided more soft particles and slightly changed the wear mechanism. Therefore, the metallic and graphene particles not only decrease the COF of the composites but also offer good wear resistance due to the creation of a friction film on the surface.

From Figure 5, we concluded that the density of Al₂O₃ ceramics decreases with increasing In content and also with the incorporation of graphene nanoplatelets. Gutierrez-Gonzalez et al. [38] reported that the densification percentage has a significant effect on the formed porosity and could lead to the GNP pullout phenomena during the wear tests and increasing wear rate. In this study, however, the wear rates of the Al₂O₃-5In-2GNP sample with lower density were higher than those of Al₂O₃ with higher density. One possible reason is due to the relief structure on the worn surface. Figures 9 and 10 give the confocal optical images and the data of the sliding track surface profiles corresponding to the line scans of Al₂O₃, Al₂O₃-5In-2GNPs, and Al₂O₃-10In-2GNPs after dry sliding. The height difference in the relief structure in the wear track profile increased after dry sliding. This means the relief structure formed on the initial surface of Al₂O₃, Al₂O₃-5In-2GNP, and Al₂O₃-10In-2GNP ceramic composites after polishing continues to increase the height difference during the dry sliding process due to the adhesion mechanism between the friction pairs.

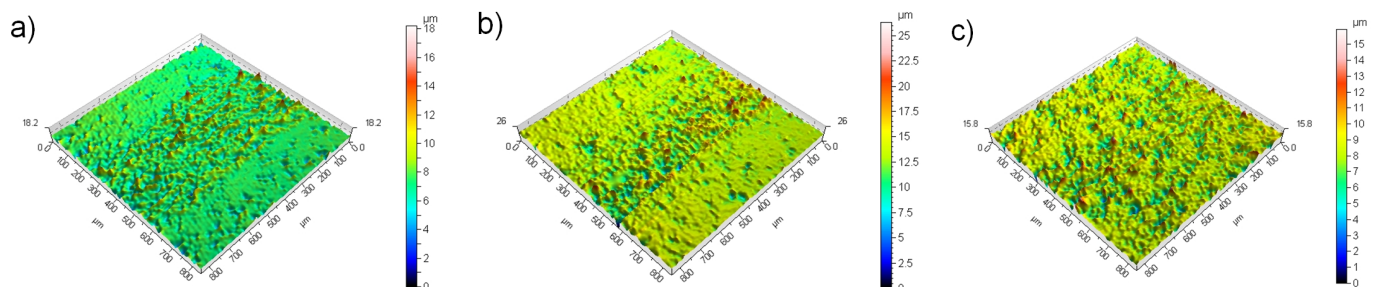


Figure 9. Axonometric plots of wear tracks on Al₂O₃ (a), Al₂O₃-5In-2GNP composite (b), and Al₂O₃-10In-2GNP composite (c) at the rotational speed of 0.1 m/s, length of 300 m and friction force of 2 N, obtained from tests under dry conditions.

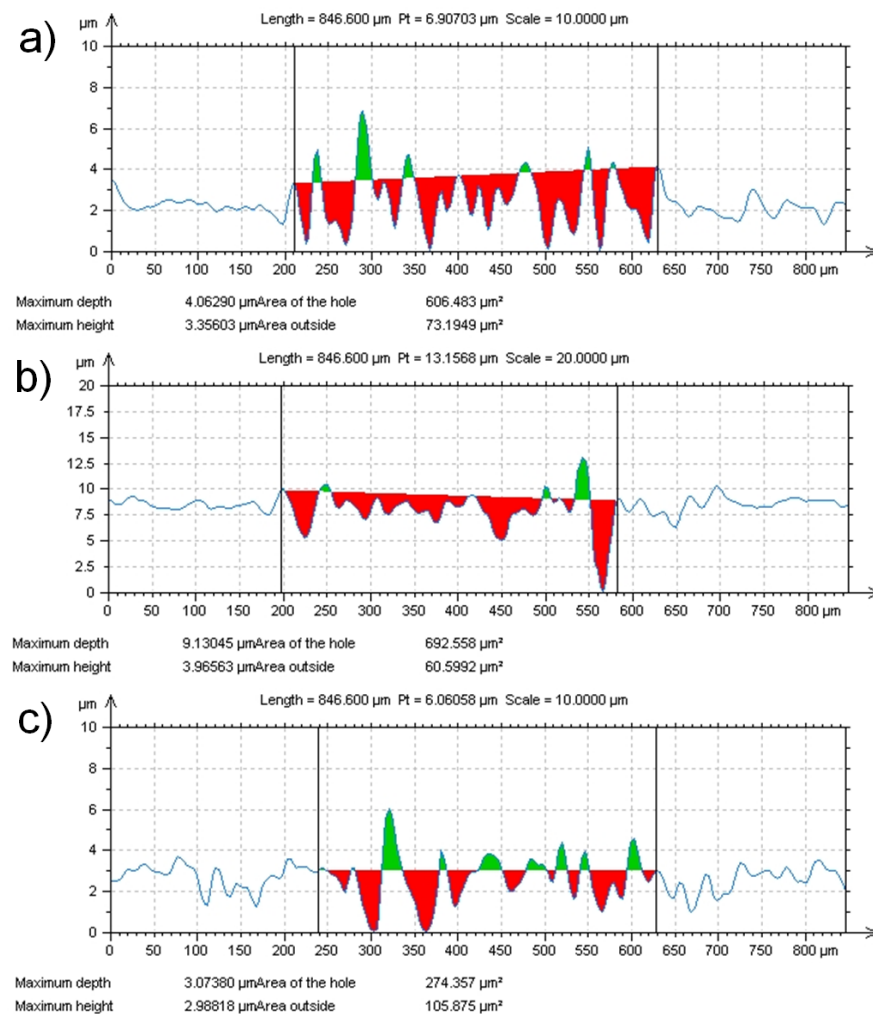


Figure 10. Profile images and the data of sliding track surface profiles corresponding to the line scans of Al_2O_3 (a), Al_2O_3 -5In-2GNP composite (b), and Al_2O_3 -10In-2GNP composite (c).

Abrasive wear particles appeared due to breaks inside the softer Al_2O_3 material against a harder SiC friction partner. By definition, the latter has a lower mechanical strength than a harder material. But fragments of the harder material were also formed (Figure 7) and they were located in the friction track. This is because, within the harder material, there are also local regions of lower strength.

Our study paid attention to the development of Al_2O_3 -In-GNP composite. As shown in the Ashby material diagram [39,40], our developed composite can be located above the metals and between technical ceramics. The sintering additives we used are present in a solid state or may form liquid phases during sintering; they were intentionally added to control the microstructural development. Numerous types of research demonstrated that minor additions of the second phase, which increase the grain boundary diffusion and surface diffusion in this system, accelerate the densification process and solve the problems with densification and brittleness [41–43]. Aluminum oxide-based ceramics have remarkable physical and chemical properties, along with good mechanical resistance and good thermal and electrical insulation properties. Despite their excellent properties, their applications are limited due to their highly fragile nature. Also, therefore, there is relevant research being carried out to improve the properties of alumina by the addition of various tough metal or ceramic binders, compared with our study in Table 1.

Table 1. Tribological and wear properties comparison of various materials tested with various parameters.

Material	COF	Wear Rate (mm ³ /m.N)	Friction Partner	Filler Content	Ref.
Al ₂ O ₃ /TiC/GPLs	0.43–0.47	1–1.5 × 10 ^{−6}	GCr15 steel ball	30 wt.% TiC, 0.2 wt.% GPLs	[41]
Al ₂ O ₃ -SiC	0.4–0.5	2–8 × 10 ^{−6}	Al ₂ O ₃ , SiC, ZrO ₂ balls	3–20 vol.% SiC	[42]
Al ₂ O ₃ /nNi	0.45	2–8 × 10 ^{−8}	Al ₂ O ₃ ball	2.5 vol.% Ni	[43]
Al ₂ O ₃ -CNF/GO	0.3–0.6	1–2 × 10 ^{−7}	Al ₂ O ₃ ball	2 vol.% CNF, 2 vol.% GO	[16]
Al ₂ O ₃ -In-GNPs	0.33–0.35	14–32 × 10 ^{−6}	SiC ball	5–10 wt.% In, 2 wt.% GNPs	Present work

4. Conclusions

Self-lubricating Al₂O₃-In-GNP composites in the form of bulk discs were fabricated by the SPS technique. Dry friction tests were carried out by sliding with a SiC ceramic ball. From the experimental results and discussion, the following conclusions can be drawn:

1. The wear rate of the ceramic matrix material rises if the amount of indium metal changes from 0 wt.% to 5 wt.% and decreases if the amount of indium metal changes from 5 wt.% to 10 wt.% in Al₂O₃-In-GNP composite samples. The wear rates can be reduced by ~45% for the Al₂O₃ ceramic matrix composite with 10 wt.% of indium metal and 2 wt.% of graphene nanoplatelets as solid lubricants compared to the monolithic sample.
2. A sintered alumina composite sample with 5 wt.% indium metal and 2 wt.% graphene nanoplatelets can reduce the average friction coefficient by about 21% compared to the monolithic alumina, while the alumina composite sample with 10 wt.% indium metal and 2 wt.% graphene nanoplatelets as solid lubricants can reduce the average friction coefficient by about 14%. The pores in sintered material can trap wear debris from the friction ball and this mechanism may have an obvious influence on the friction coefficient value under the present conditions.
3. The mechanism for improving the tribological properties of alumina composite materials is that the indium metal and graphene nanoplatelets incorporated into the matrix can act as a lubricant store for creating a friction film and also on a smaller scale can capture wear debris, which could play an important role in promoting the engineering applications of Al₂O₃-In-GNP self-lubricating composite materials.

Author Contributions: Conceptualization, V.P.; methodology, V.P.; validation, V.P., M.P. and L.F.; formal analysis, V.P. and R.S.; investigation, V.P., R.D. and F.K.; data curation, V.P.; writing—original draft preparation, V.P. and M.P.; writing—review and editing, V.P. and R.S.; visualization, V.P.; supervision, J.D.; project administration, V.P.; funding acquisition, V.P. All authors have read and agreed to the published version of the manuscript.

Funding: This work was supported by the Scientific Grant Agency of the Ministry of Education, Science, Research and Sport of the Slovak Republic and the Slovak Academy of Sciences, projects: VEGA 2/0113/23 and VEGA 2/0114/23. The research was also supported by the Slovak Research and Development Agency under Contract Nos.: APVV-20-0303 and APVV-21-0180. The research was also carried out within the framework of the project: Research Centre of Advanced Materials and Technologies for Recent and Future Applications “PROMATECH”, ITMS project code: 26220220186, which is supported by the Operational Program “Research and Development” financed through the European Regional Development Fund.

Institutional Review Board Statement: Not applicable.

Informed Consent Statement: Not applicable.

Data Availability Statement: Data are contained within the article.

Conflicts of Interest: The authors declare no conflicts of interest. The funders had no role in the design of the study; in the collection, analyses, or interpretation of data; in the writing of the manuscript; or in the decision to publish the results.

References

1. Surappa, M.K. Aluminium matrix composites: Challenges and opportunities. *Sadhana* **2003**, *28*, 319–334. [[CrossRef](#)]
2. Zhang, C.; Nieto, A.; Agarwal, A. Ultrathin graphene tribofilm formation during wear of Al₂O₃–graphene composites. *Nanomater. Energy* **2016**, *5*, 1–9. [[CrossRef](#)]
3. Ramirez, C.; Figueiredo, F.M.; Miranzo, P.; Poza, P.; Osendi, M.I. Graphene nanoplatelet/silicon nitride composites with high electrical conductivity. *Carbon* **2012**, *50*, 3607–3615. [[CrossRef](#)]
4. Fan, Y.; Wang, L.; Li, J. Preparation and electrical properties of graphene nanosheet/Al₂O₃ composites. *Carbon* **2010**, *48*, 1743–1749. [[CrossRef](#)]
5. Centeno, A.; Rocha, V.G.; Alonso, B. 2013 Graphene for tough and electroconductive alumina ceramics. *J. Eur. Ceram. Soc.* **2013**, *33*, 3201–3210. [[CrossRef](#)]
6. Porwal, H.; Tatarko, P.; Saggarr, R.; Grasso, S.; Kumar Mani, M.; Dlouhý, I.; Dusza, J.; Reece, M.J. Tribological properties of silica-graphene nano-platelet composites. *Ceram. Int.* **2014**, *40*, 12067–12074. [[CrossRef](#)]
7. Rutkowski, P.; Stobierski, L.; Zientara, D.; Jaworska, L.; Klimczyk, P.; Urbanik, M. The influence of the graphene additive on mechanical properties and wear of hot-pressed Si₃N₄ matrix composites. *J. Eur. Ceram. Soc.* **2015**, *35*, 87–94. [[CrossRef](#)]
8. Li, H.; Xie, Y.; Li, K.; Huang, L.; Huang, S.; Zhao, B.; Zheng, X. Microstructure and wear behavior of graphene nanosheets-reinforced zirconia coating. *Ceram. Int.* **2014**, *40*, 12821–12829. [[CrossRef](#)]
9. Balko, J.; Hvizdos, P.; Dusza, J.; Balazsi, C.; Gamcova, J. Wear damage of Si₃N₄-graphene nanocomposites at room and elevated temperatures. *J. Eur. Ceram. Soc.* **2014**, *34*, 3309–3317. [[CrossRef](#)]
10. Belmonte, M.; Ramirez, C.; Gonzalez-Julian, J.; Schneider, J.; Miranzo, P.; Osendi, M.I. The beneficial effect of graphene nanofillers on the tribological performance of ceramics. *Carbon* **2013**, *61*, 431–435. [[CrossRef](#)]
11. Hvizdos, P.; Dusza, J.; Balazsi, C. Tribological properties of Si₃N₄-graphene nanocomposites. *J. Eur. Ceram. Soc.* **2013**, *33*, 2359–2364. [[CrossRef](#)]
12. Berman, D.; Erdemir, A.; Sumant, A.V. Few layer graphene to reduce wear and friction on sliding steel surfaces. *Carbon* **2013**, *54*, 454–459. [[CrossRef](#)]
13. Kim, H.J.; Lee, S.M.; Oh, Y.S.; Yang, Y.H.; Lim, Y.S.; Yoon, D.H.; Lee, C.; Kim, J.Y.; Ruoff, R.S. Unoxidized graphene/alumina nanocomposite: Fracture-and wear-resistance effects of graphene on alumina matrix. *Sci. Rep.* **2014**, *4*, 5176. [[CrossRef](#)] [[PubMed](#)]
14. Kim, K.S.; Lee, H.J.; Lee, C.; Lee, S.K.; Jang, H.; Ahn, J.H.; Kim, J.H.; Lee, H.J. Chemical Vapor Deposition-Grown Graphene: The Thinnest Solid Lubricant. *ACS Nano* **2011**, *5*, 5107–5114. [[CrossRef](#)] [[PubMed](#)]
15. Lee, C.; Li, Q.; Kalb, W.; Liu, X.Z.; Berger, H.; Carpick, R.W.; Hone, J. Frictional Characteristics of Atomically Thin Sheets. *Science* **2010**, *328*, 76–80. [[CrossRef](#)] [[PubMed](#)]
16. Gutiérrez-Mora, F.; Cano-Crespo, R.; Rincón, A.; Moreno, R.; Domínguez-Rodríguez, A. Friction and wear behavior of alumina-based graphene and CNFs composites. *J. Eur. Ceram. Soc.* **2017**, *37*, 3805–3812. [[CrossRef](#)]
17. Huang, T.; Xin, Y.; Li, T.; Nutt, S.; Su, C.; Chen, H.; Liu, P.; Lai, Z. Modified graphene/polyimide nanocomposites: Reinforcing and tribological effects. *ACS Appl. Mater. Interfaces* **2013**, *5*, 4878–4891. [[CrossRef](#)]
18. Ren, G.; Zhang, Z.; Zhu, X.; Ge, B.; Guo, F.; Men, X.; Liu, W. Influence of functional graphene filler on the tribological behaviors of Nomex fabric/phenolic composite. *Compos. Part A* **2013**, *49*, 157–164. [[CrossRef](#)]
19. Tabandeh-Khorshid, M.; Omrani, E.; Menezes, P.L.; Rohatgi, P.K. Tribological performance of self-lubricating aluminum matrix nanocomposites: Role of graphene nanoplatelets. *Eng. Sci. Technol. Int. J.* **2016**, *19*, 463–469. [[CrossRef](#)]
20. Rohatgi, P.K.; Tabandeh-Khorshid, M.; Omrani, E.; Lovell, M.R.; Menezes, P.L. Tribology of Metal Matrix Composites. In *Tribology for Scientists and Engineers*; Menezes, P.L., Nosonovsky, M., Ingole, S., Kailas, S., Lovell, M., Eds.; Springer: New York, NY, USA, 2013; pp. 233–268, ISBN 978-1-4614-1945-7. [[CrossRef](#)]
21. Omrani, E.; Rohatgi, P.K.; Menezes, P.L. *Tribology and Applications of Self-Lubricating Materials*, 1st ed.; CRC Press: Boca Raton, FL, USA, 2017; ISBN 9781315154077. [[CrossRef](#)]
22. Kasar, A.K.; Menezes, P.L. Friction and wear behavior of alumina composites with in-situ formation of aluminum borate and boron nitride. *Materials* **2020**, *13*, 4502. [[CrossRef](#)]
23. Furlan, K.P.; Gonçalves, P.D.C.; Consoni, D.R.; Dias, M.V.G.; De Lima, G.A.; de Mello, J.D.B.; Klein, A.N. Metallurgical Aspects of Self-lubricating Composites Containing Graphite and MoS₂. *J. Mater. Eng. Perform.* **2017**, *26*, 1135–1145. [[CrossRef](#)]
24. Kelly, P.; Arnell, R. Magnetron sputtering: A review of recent developments and applications. *Vacuum* **2000**, *56*, 159–172. [[CrossRef](#)]
25. Quazi, M.M.; Fazal, M.A.; Haseeb, A.S.M.A.; Yusof, F.; Masjuki, H.H.; Arslan, A. A Review to the Laser Cladding of Self-Lubricating Composite Coatings. *Lasers Manuf. Mater. Process.* **2016**, *3*, 67–99. [[CrossRef](#)]
26. Zhang, S.; Zhou, J.; Guo, B.; Zhou, H.; Pu, Y.; Chen, J. Friction and wear behavior of laser cladding Ni/hBN self-lubricating composite coating. *Mater. Sci. Eng. A* **2008**, *491*, 47–54. [[CrossRef](#)]
27. Wang, H.M.; Yu, R.L.; Li, S.Q. Microstructure and tribological properties of laser clad NiO/Al₂O₃ self-lubrication wear-resistant ceramic matrix composite coatings. *Mocaxue Xuebao (Tribol.) (China)* **2002**, *22*, 157–160.
28. Huang, B.; Zhang, C.; Zhang, G.; Liao, H. Wear and corrosion resistant performance of thermal-sprayed Fe-based amorphous coatings: A review. *Surf. Coat. Technol.* **2019**, *377*, 124896. [[CrossRef](#)]
29. Chen, X.; Peng, Z.; Yu, X.; Fu, Z.; Yue, W.; Wang, C. Microstructure and tribological performance of self-lubricating diamond/tetrahedral amorphous carbon composite film. *Appl. Surf. Sci.* **2011**, *257*, 3180–3186. [[CrossRef](#)]

30. Kalss, W.; Reiter, A.; Derflinger, V.; Gey, C.; Endrino, J. Modern coatings in high performance cutting applications. *Int. J. Refract. Met. Hard Mater.* **2006**, *24*, 399–404. [[CrossRef](#)]
31. Sahin, Y.; Sur, G. The effect of Al₂O₃, TiN and Ti (C,N) based CVD coatings on tool wear in machining metal matrix composites. *Surf. Coat. Technol.* **2004**, *179*, 349–355. [[CrossRef](#)]
32. Niu, M.; Bi, Q.; Yang, J.; Liu, W. Tribological performance of a Ni₃Al matrix self-lubricating composite coating tested from 25 to 1000 °C. *Surf. Coat. Technol.* **2012**, *206*, 3938–3943. [[CrossRef](#)]
33. Shi, X.; Song, S.; Zhai, W.; Wang, M.; Xu, Z.; Yao, J.; Din, A.Q.U.; Zhang, Q. Tribological behavior of Ni₃Al matrix self-lubricating composites containing WS₂, Ag and hBN tested from room temperature to 800 °C. *Mater. Des.* **2014**, *55*, 75–84. [[CrossRef](#)]
34. Zhu, S.; Bi, Q.; Yang, J.; Liu, W.; Xue, Q. Ni₃Al matrix high temperature self-lubricating composites. *Tribol. Int.* **2011**, *44*, 445–453. [[CrossRef](#)]
35. John, M.; Menezes, P.L. Self-Lubricating Materials for Extreme Condition Applications. *Materials* **2021**, *14*, 5588. [[CrossRef](#)] [[PubMed](#)]
36. Puchý, V.; Hvizdoš, P.; Ivor, M.; Medved', D.; Hnatko, M.; Kovalčíková, A.; Sedlák, R.; Dusza, J. Preparation, friction, wear, and fracture of the Si₃N₄-Ag-GNPs composites prepared by SPS. *J. Eur. Ceram. Soc.* **2020**, *40*, 4853–4859. [[CrossRef](#)]
37. Wardzinski, B.; Buttery, M.; Roberts, E. The potential of indium as a soft metal lubricant replacement for lead. In *'15th European Space Mechanisms & Tribology Symposium—ESMATS 2013' Noordwijk, The Netherlands, 25–27 September 2013*; Ouwehand, L., Ed.; ESA-SP: Noordwijk, The Netherlands, 2013; Volume 718, p. 32, ISBN 978-92-9221-282-7.
38. Gutierrez-Gonzalez, C.F.; Smirnov, A.; Centeno, A.; Fernández, A.; Alonso, B.; Rocha, V.G.; Torrecillas, R.; Zurutuza, A.; Bartolome, J.F. Wear behavior of graphene/alumina composite. *Ceram. Int.* **2015**, *41*, 7434–7438. [[CrossRef](#)]
39. Sun, J.; Zhao, J.; Huang, Z.; Yan, K.; Shen, X.; Xing, J.; Gao, Y.; Jian, Y.; Yang, H.; Li, B. A Review on Binderless Tungsten Carbide: Development and Application. *Nano-Micro Lett.* **2020**, *12*, 13. [[CrossRef](#)] [[PubMed](#)]
40. Ashby, M.F. *The CES EduPack Resource Booklet 2: Material and Process Selection Charts*; Granta Design Limited: Cambridge, UK, 2009.
41. Wang, J.; Cheng, Y.; Zhang, Y.; Yin, Z.; Hu, X.; Yuan, Q. Friction and wear behavior of microwave sintered Al₂O₃/TiC/GPLs ceramic sliding against bearing steel and their cutting performance in dry turning of hardened steel. *Ceram. Int.* **2017**, *43*, 14827–14835. [[CrossRef](#)]
42. Parchovianský, M.; Balko, J.; Švančárek, P.; Sedláček, J.; Dusza, J.; Lofaj, F.; Galusek, D. Mechanical properties and sliding wear behaviour of Al₂O₃-SiC nanocomposites with 3–20 vol% SiC. *J. Eur. Ceram. Soc.* **2017**, *37*, 4297–4306. [[CrossRef](#)]
43. Rodriguez-Suarez, T.; Bartolomé, J.; Smirnov, A.; Lopez-Esteban, S.; Torrecillas, R.; Moya, J. Sliding wear behaviour of alumina/nickel nanocomposites processed by a conventional sintering route. *J. Eur. Ceram. Soc.* **2011**, *31*, 1389–1395. [[CrossRef](#)]

Disclaimer/Publisher's Note: The statements, opinions and data contained in all publications are solely those of the individual author(s) and contributor(s) and not of MDPI and/or the editor(s). MDPI and/or the editor(s) disclaim responsibility for any injury to people or property resulting from any ideas, methods, instructions or products referred to in the content.